Physics-Based Approach to Geometry-Insensitive Recovery of Quantitative Scene Parameters from Images

S. J. Preece and E. Claridge

School of Computer Science, University of Birmingham, Edgbaston, Birmingham, B15 2TT, UK

(sjp,exc)@cs.bham.ac.uk

Abstract

By defining appropriate optical filters it is possible to recover quantitative parameters which determine colouration of a class of objects irrespective of scene geometry and intensity of illuminating light. A relationship between scene parameters and their spectra is established from a forward model of light transport. Optimal spectral filters which minimise the error of the inverse mapping are then sought. To achieve geometric and illumination invariance, optimisation is based on image quotients and not on image values. When applied to human skin imaging, the technique is able to recover histological parameters to an accuracy adequate for clinical use.

1. Introduction

Physics-based approaches to computer vision have recently become increasingly popular. In contrast to traditional image analysis techniques, which analyse the final image, physics-based approaches rely on a fundamental understanding of the image formation process. This process consists of an involved series of interactions of the illuminating light at, and within, object surfaces. Using an understanding of these interactions relationships between scene parameters and image values are established. Physics based approaches have been shown to be successful in many different areas of image understanding, such as obtaining shape from shading[1] and removing the effects of variations in illumination prior to image segmentation.[2]

The approach described in this article is applicable to problems in which a small number of parameters can be used to describe every potential object/object characteristic within an imaged scene. For example a medical image system may be required to analyse a particular tissue. The underlying structure of the tissue will not vary, only specific characteristics such

as thickness of the different layers or the concentration of a particular chemical constituent. In this situation a small parameter vector would be able to describe all possible variations in the characteristics of the imaged scene.

The aim of the research is to establish a mapping between the vector of image values, recorded at each pixel, and the vector of parameter values. This mapping should be insensitive to both scene geometry and intensity of the incident illumination. The mapping must be established for all possible parameter vectors, thus enabling scene parameters to be recovered from image data. In a previous publication[3] problems of 2D recognition and measurement, where the illumination intensity is known, were analysed. It was shown that, in order to maximise the accuracy of parameter recovery, it is necessary to choose specific optical filters for image acquisition. This idea is developed further in this article. It is again shown that specific optical filters are required if a mapping, between image values and the vector of parameter values, is to be established which is insensitive to both geometry and the intensity of the incident illumination.

In the following section the dichromatic reflection model is reviewed and an outline of the problem presented. Previous work on illumination invariance and geometry-insensitive recognition is then discussed within the context of the current problem. In section 4 a detailed mathematical formulation of the problem is presented. From this formulation an optimisation criterion is established which enables an appropriate mapping to be defined. An example problem, the imaging of human skin, is then discussed. It is shown that an objectively defined set of optical filters can be used to recover histological parameters to within a relatively small uncertainty.

2. Dichromatic Reflection Model

Most physics-based approaches used in computer vision employ what is known as the dichromatic model.[4] This states that light remitted from an object is the sum of two components, the "body" component and the "surface" component. The body component refers to physical processes occurring after penetration of light into the material and the surface term to reflections which take place at the surface of the object. The body component is a function of the spectral characteristics of the object, whereas the surface component depends only on the object geometry and the incident light. The theory states further that each component can be considered the product of a geometrical term and a wavelength dependent term. Light remitted from an object is measured using a digital camera with a small number of optical filters. Image values, for image location (x, y), corresponding to the nth filter are given by

$$\begin{aligned} i^n(x,y) &= K_b C_b^n + K_s C_s^n \\ &= K_b \int E(\lambda) S(\lambda) R^n(\lambda)\, d\lambda + K_s \int E(\lambda) R^n(\lambda)\, d\lambda \end{aligned} \tag{1}$$

where K_b and K_s are the geometric terms of the body and surface component respectively and C_b^n and C_s^n are colour terms. The first integral is the product of three terms: $E(\lambda)$ is the illuminating light, $S(\lambda)$ the spectral remittance from the body of the imaged object and $R^n(\lambda)$ the spectral response of the nth optical filter. In the second integral there are only two terms as there is no wavelength dependence on the surface component of reflection. The dichromatic reflection model is very important for 3-D scene analysis[5,6] as it allows for both colour and geometrical analysis of objects within a scene. The approach presented in this article will be restricted to problems in which the surface term in equation (1) can be neglected. Although this will limit the class of problems to scenes containing objects which do not have a specular component of reflection, such as many organic objects, image processing algorithms have been developed to remove this component of reflection. For example, it has been shown that it is possible to remove the highlights from complex images containing inhomogeneous dielectrics.[7] It is also possible to remove the surface component of reflection using a polarising filter. Once this component has been removed from image data, it will be possible to use the techniques described in this paper.

A key issue is to show that the methodology is valid for problems where the intensity of the illuminating light is unknown. For this purpose the incident light is written as

$$E(\lambda) = \epsilon_0 E_0(\lambda) \tag{2}$$

where ϵ_0 is a wavelength independent scaling factor. Equation (1) now becomes

$$i^n(x,y) = \epsilon \int E_0(\lambda) S(\lambda) R^n(\lambda)\, d\lambda \tag{3}$$

where $\epsilon = \epsilon_0 K_b$. A digital camera records a N-dimensional vector of image values at each location (x,y). If a mapping, which is independent of the constant ϵ, can be established between the vector of image values and the vector of parameters, then it will be possible to recover scene parameters from image data in a way that does not depend on illumination intensity or scene geometry. In this paper a methodology is presented which enables such mapping to be defined. Before this is discussed it it useful to briefly review related work.

3. Review of Previous Work on Illumination Invariance

There has been substantial work carried out to develop image analysis algorithms which are able to identify different objects irrespective of the illuminating light. Many of the techniques developed are based around the linear model of surface reflectance first proposed by Maloney and Wandell.[8] This approach is based on the idea that the surface reflectance of any object within the imaged scene can be expressed as a weighted sum of basis spectral reflectance functions

$$S(\lambda) = \sum_{j=1}^{n} \sigma_j S_j(\lambda) \tag{4}$$

and that the illuminating light can similarly be expressed as a weighted sum of basis lights. It has been shown that only a small number of basis functions are required to obtain accurate approximations to the surface reflectances of many naturally occuring objects[8] and also the spectral variation of natural daylight.[9] With this technique it is possible to recover the vector of weighting constants σ_j from a vector of image values and thus specify the spectral reflectance of the imaged object at every pixel. Every potential imaged object/object characteristic will have a unique spectral reflectance. Thus, if the spectral reflectance can be determined using the linear model (4), then the parameter vector can be specified. With this approach it should be possible to recover a parameter vector from the vector of image values at each pixel. Unfortunately the method is only able to recover the weighting constants σ_j to within a mulitplicative scaling factor[8] and thus can not be used to specify the exact spectral reflectance and therefore the exact parameter vector (See section 4).

An approach to geometry-insensitive segmentation of images has been developed by Healey[10] based on the idea of normalised colour. With this approach image values are first divided by an estimate of normalised colour. This estimate is based on approximating the incoming signal from colour pixel values by using a finite-dimensional linear approximation to represent the colour signal.[11–13] Using these normalised values different metal and dielectirc materials could be identified across an imaged scene in which the geometry varied considerably. A similar technique was also used by Afromowitz *et al.*[14,15] to evaluate burn injuries. In this case, RGB image values were normalised by dividing them by the response of an IR filter. From the normalised values it was possible to assess the extent of burn damage across a given area of imaged skin.

In this paper the idea of normalised colour is adapted to define the concept of an image quotient, obtained by dividing one image value, calculated from equation (3), by another. For a given image vector the nth image quotient is given as

$$\bar{i}^{\bar{n}} = \frac{i^n}{i^m} \qquad n \neq m. \tag{5}$$

Simple consideration of equation (3) shows that any quotient defined in this way will be invariant to a change in the parameter ϵ. Thus any method for the recovery of parameter values from image quotients will be independent of scene geometry and illumination intensity.

4. Formulation of the Problem

This approach is fundamentally different from most other work related to colour constancy. The goal there is to remove the effect of geometry and illumination prior to either segmentation or pixel or object classification. Both these tasks require that pixels belonging to a particular class or object are statistically similar. The operations to remove the dependency on geometry and illuminating light change colour representation such that pixels are now

clustered on the basis of similarity of their intrinsic surface colouration. The objective here is to extract quantitative parameters upon which the object colouration depends, not to find statistical similarities. Moreover, the specific filters are chosen to maximise the distance in the image quotient space between vectors corresponding to similar parameter values, as this minimises the error on the parameter value recovered from the colour image.

The technique described will only be applicable to scenes in which a small number of parameters are required to describe all possible objects/object characteristics. In the formulation the parameters will be considered to vary continously. Thus, the technique will be particularly applicable to problems where object characteristics need to be measured across an image. For K scene parameters the parameter vector is defined as,

$$\mathbf{p} = \sum_{k=1}^{K} p_k \qquad \mathbf{p} \in \mathbf{P} \tag{6}$$

and the space $\mathbf{P}$ defines all potential object characteristics. Ultimately, a mapping from image quotients back to the parameter vector is required, but first the forward problem of obtaining image quotients for a given parameter vector is considered. A reflectance spectrum, corresponding to a given point within parameter space, can be described by the vector in M dimensional wavelength space

$$\lambda = \sum_{m=1}^{M} \lambda_m \qquad \lambda \in \mathbf{\Lambda} \tag{7}$$

where the space $\mathbf{\Lambda}$ defines all possible spectral reflectance functions. The mapping a defined as

$$a : \mathbf{P} \longrightarrow \mathbf{\Lambda} \tag{8}$$

is introduced to denote the mapping from parameter space to wavelength space. This mapping gives the spectral reflectance of the object specified by the vector $\mathbf{p}$. Such a mapping can be achieved either by a spectroscopic measurement, or by using a mathematical model which takes as input the parameters and produces a corresponding reflectance spectrum. Models of light propagation in different media, such as the Monte Carlo method[16] or the Kubelka Munk approximation[17] can be used for this purpose. It must be possible to perform this mapping across the whole of parameter space, thus defining every possible spectral reflectance function.

A digital camera with N optical filters records a N dimensional image vector at each pixel. The image vector is given as

$$\mathbf{i} = \sum_{n=1}^{N} i^n \qquad \mathbf{i} \in \mathbf{I} \tag{9}$$

where $\mathbf{I}$ describes the space of all possible image values. The process of image acquisition can be considered as the projection of points in wavelength space to points in filter space.

This projection is performed by the mapping function

$$b : \mathbf{\Lambda} \longrightarrow \mathbf{I}. \tag{10}$$

Equation (3) performs mapping b in continuous form. In discrete form, the response of the nth optical filter, is given as

$$i^n = \epsilon \sum_{m=1}^{M} R_m^n \lambda_m \tag{11}$$

where $\lambda_m = E_0(\lambda)S(\lambda)$ and the positive weights at each wavelength are given by R_m^n, thus defining each filter response function. A digital camera effectively performs mapping b, projecting points from a large dimensional space (wavelength space) to a small dimensional space (filter space). With such a mapping there will be a substantial loss of information. Even with this loss of information, it should be possible to define the mapping in such a way that accurate information regarding the original parameter values can still be recovered from image data. Conditions for this mapping will be discussed in the following section. Most current image acquisition systems use an RGB system of filters. Although this defines a potential mapping b, it may not be the best mapping with which to recover parameter values from image data. Indeed, it has been shown by the authors in previous work,[3] that an objectively defined set of optical filters is able to perform the task of recovery of parameters, which describe the variation in human skin, better than a standard RGB system.

Once the vector of image values has been obtained, a vector of image quotients can be calculated using equation (5). The vector of image quotients is given as

$$\bar{\mathbf{i}} = \sum_{\bar{n}=1}^{\bar{N}} \bar{i}^{\bar{n}} \qquad \bar{\mathbf{i}} \in \bar{\mathbf{I}} \tag{12}$$

where $\bar{\mathbf{I}}$ describes the space of all possible image quotients. The mapping from filter space to the space of image quotients is performed after image acquisition and will be referred to as mapping c, defined as

$$c : \mathbf{I} \longrightarrow \bar{\mathbf{I}}. \tag{13}$$

There are many ways to define the image quotients and thus the mapping c. For example, pairs of image values could be used to define image quotients as

$$\bar{i}^{\bar{n}} = \frac{i_{2n-1}}{i_{2n}} \qquad n = 1, 2, ..., \frac{N}{2} \tag{14}$$

or a single image value could be taken as the denominator with which to calculate image quotients from the remaining image values, for example

$$\bar{i}^{\bar{n}} = \frac{i_n}{i_1} \qquad n = 2, 3, ..., N. \tag{15}$$

At most the dimensionality, $\bar{N}$, of the new space will be one less that that of the original filter space, N. This would correspond to the definition given in (15). Alternatively, if the image quotients were defined as given in (14), then the dimensionality of the new space will be half that of the original filter space. The the aim is to recover a K dimensional parameter vector from $\bar{N}$ image quotients. Thus there must be at least as many image quotients as parameters, that is, $\bar{N} \geq K$.

The function f defined as

$$f = a \circ b \circ c \qquad f : \mathbf{P} \longrightarrow \bar{\mathbf{I}} \tag{16}$$

represents the three stage mapping from parameter space to wavelength space, to image space, and finally to the space of image quotients. For a given set of optical filters, it will be possible to perfom this mapping across the whole of parameter space, provided it is possible to obtain a spectrum for any given parameter vector. The inverse of function f is defined as

$$f^{-1} : \bar{\mathbf{I}} \longrightarrow \mathbf{P} \tag{17}$$

and maps from the space of image quotients directly to parameter space. If it is possible to define an appropriate f^{-1}, it will be possible to recover parameter values from image data in a way that is independent of illumination intensity and scene geometry. The ultimate aim is to find the optimum f^{-1} which maximises the accuracy of parameter recovery. Before a detailed discussion of this mapping is presented, it is important to emphasise that the form of the function f will depend on the mappings a, b and c. Although mapping a is fixed for a given problem, mapping b will vary with the choice of optical filters and mapping c will vary depending on how the image quotients are defined.

5. Defining an optimum mapping function

Any mapping function which is to map from the space of image quotients ($\bar{\mathbf{I}}$-space) to parameter space ($\mathbf{P}$-space) must be 1-1. That is, for a given point in $\mathbf{P}$-space, there must be a corresponding unique point in $\bar{\mathbf{I}}$-space and vice-versa. If this is not the case, ambiguity will arise as it could be possible to recover more that one set of parameter values from a given vector of image quotients. Once this condition has been established, it is necessary to consider the error associated with paramter recovery. Using a digital camera it will only be possible to obtain image values to within a given uncertainty. This will introduce an uncertainty into the final recovery of the parameter vector. There could also be an error associated with the prediction/measurement of a spectrum from the parameter vector. For simplicity the analysis presented in this article will be restricted to problems in which the error associated with the spectral measurement can be neglected. It is hoped that future analysis will allow this error to be taken into consideration.

Initially the problem where one parameter is sufficient to describe all variation in an imaged scene will be analysed. The methodology will then be extended to problems where the number of parameters is greater than one. Consider the case where one image quotient (two image values) are used to recover a single parameter value.

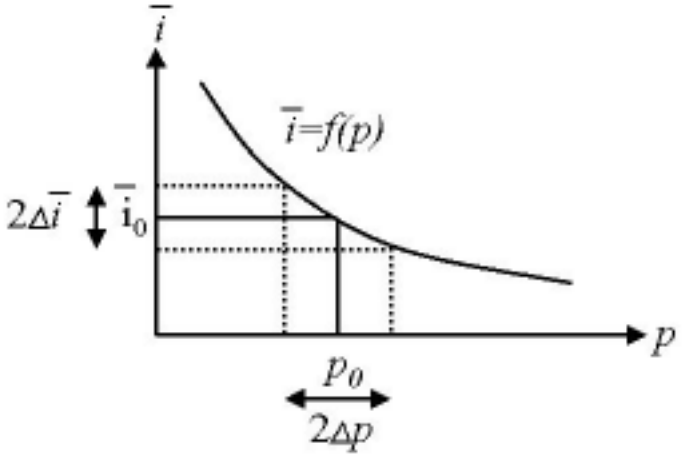

Fig. 1. Plot of single image quotient vs single parameter value

Figure 1 illustrates a function f which gives the image quotient as a function of the parameter p. It is clear that in order to satisfy the 1-1 condition, the curve must not have any turning points, that is, it must increase or decrease monotonically in the appropriate range of p. Mathematically this is expressed as

$$\left|\frac{df}{dp}\right| > 0 \qquad \forall p \in P. \tag{18}$$

Measurement of an image quotient value $\bar{i}_0$, corresponding to a parameter value p_0, is now considered. Associated with acquistion of each image value is an uncertainty due to camera error. It is straightforward to show, using standard error analysis, that the error associated with an image quotient $\bar{i}$, which has been calculated from the two image values i_1 and i_2, is given as

$$\Delta\bar{i} = \Delta i \left(\frac{i_1 + i_2}{i_2^2 - (\Delta i)^2}\right) \tag{19}$$

where Δi is the camera uncertainty. This error has been shown on the ordinate of the graph in figure 1. If the derivate of f is non-zero in some neighbourhood of p_0 then it is possible to approximate this function linearly. Assuming the error Δi to lie within this neighbourhood,

the corresponding error in the parameter value is given as

$$\Delta p = \Delta \bar{i} / \frac{df}{dp}. \tag{20}$$

Thus, it is possible to obtain a value for the error Δp, associated with parameter recovery, at any point in **P**-space. An optimisation criterion can then be defined based on some measure of this error. For most applications it will be necessary to minimise the error equally across the whole of **P**-space. For others it may be that high accuracy parameter recovery is required within a certain range of parameter values. For example, in a medical image application, imaged tissue could be deemed pathological once a characterising parameter changes beyond a threshold level. This would need to be accounted for with some form of weighting in the optimisation criterion. It is interesting to note that in order to minimse Δp, it is necessary to maximise the magnitude of the derivative given in equation (18). This will ensure that any search, carried out to find an optimum f, will tend to move towards regions of search space where the 1-1 condition is satisfied.

In theory it is possible to recover the parameter using more than one image quotient. In this case it will be necessary to calculate the error associated with parameter recovery for each of the image quotients and select the one, at each point in **P**-space, which has the smallest associated error (Δp). It may be that the optimisation procedure gives a single image quotient which performs better than any other across the whole of **P**-space. In this situation there is no benefit to using more that one image quotient.

The analysis is now extended to the general problem where the recovery of a K dimensional parameter vector is required from an $\bar{N}$ dimensional vector of image quotients. Initially the analysis will be restricted to the case where $\bar{N} = K$ and will then be extended to include situations where $\bar{N} > K$. As discussed earlier, if $\bar{N} < K$, then it is not possible to recover K dimensional data from an $\bar{N}$ dimensional measurement.

The mapping function **f**, defined as

$$\bar{\mathbf{i}} = \mathbf{f}(\mathbf{p}) \tag{21}$$

must now be considered a vector valued function of a vector variable. In the following analysis specific results from differential geometry will be used. For further details the reader is directed to an appropriate text, for example Lipschutz.[19] To establish whether the function **f** is 1-1 it is first necessary to consider the behaviour of the determinant of the Jacobian matrix, simply referred to as the Jacobian. This is defined as

$$det\left(\frac{\partial f_n}{\partial p_k}\right) = \begin{vmatrix} \frac{\partial f_1}{\partial p_1} & \frac{\partial f_1}{\partial p_2} & \cdots & \frac{\partial f_1}{\partial p_k} \\ \cdots & \cdots & \cdots & \cdots \\ \frac{\partial f_n}{\partial p_1} & \frac{\partial f_n}{\partial p_2} & \cdots & \frac{\partial f_n}{\partial p_k} \end{vmatrix}. \tag{22}$$

The Jacobian can be considered the multidimensional equivalent of the one dimensional derivative given in equation (18). The inverse function theorem[19] states that, if the Jacobian is non-zero at a point $\mathbf{p_0}$ in $\mathbf{P}$-space, then there exists a neighbourhood around $\mathbf{p_0}$ where the function $\mathbf{f}$ can be approximated linearly as

$$\mathbf{f}(\mathbf{p}) = \mathbf{f}(\mathbf{p_0}) + d\mathbf{f}(\mathbf{p_0})(\mathbf{p} - \mathbf{p_0}) \tag{23}$$

where $d\mathbf{f}$ is the differential of $\mathbf{f}$ and is given as

$$d\mathbf{f} = \frac{\partial \mathbf{f}}{\partial p_1} dp_1 + \frac{\partial \mathbf{f}}{\partial p_2} dp_2 + \cdots + \frac{\partial \mathbf{f}}{\partial p_k} dp_k. \tag{24}$$

It follows that in this neighbourhood the function $\mathbf{f}$ is 1-1. Thus, if it is possible to establish that the Jacobian is strictly positive or strictly negative throughout the whole of $\mathbf{P}$-space, the function $\mathbf{f}$ will be 1-1 everywhere. Once this condition has been established, it is necessary to consider how the error associated with image acquisition maps under $\mathbf{f}^{-1}$, to give the corresponding error in parameter recovery. The error associated with each image quotient is calculated using equation (19). The combination of errors maps out a hypervolume in $\bar{\mathbf{I}}$-space, centred on the point $\mathbf{i_0}$. This has been illustrated in figure 2 for the case of a 2D $\mathbf{P}$-space, where an ellipse is obtained or a circle if the errors are equal. An ellipsoid is obtained in 3D space and a hyperellipse in higher dimensions. Although the following analysis will be based on a 2D $\mathbf{P}$-space, the arguments are equally valid in higher dimensions.

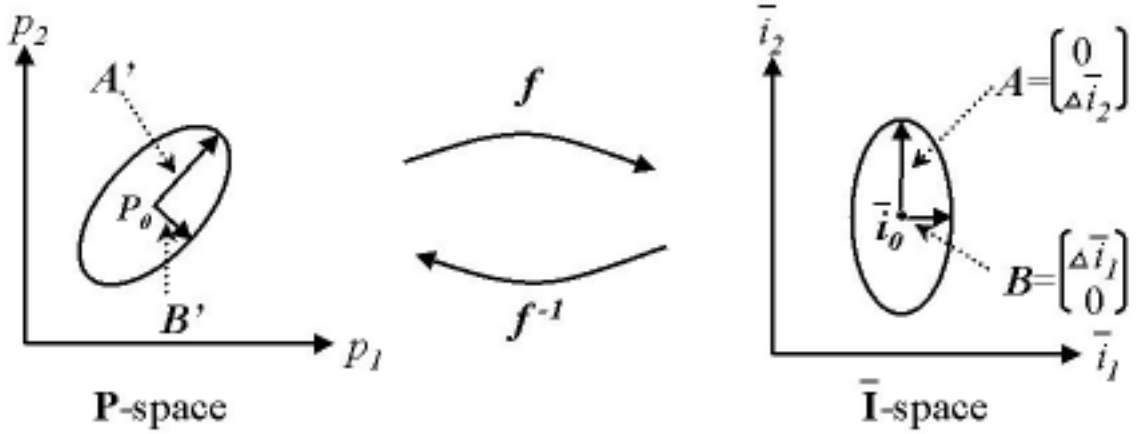

Fig. 2. Diagram showing the mapping $\mathbf{f}$ from paramter space to the space of image quotients

The ellipse in $\bar{\mathbf{I}}$-space represents all possible image quotient vectors which could correspond to a camera measurement $\bar{\mathbf{i}} = \bar{\mathbf{i}}_0$. It is assumed that the region of error lies within the neighbourhood of $\bar{\mathbf{i}} = \bar{\mathbf{i_0}}$ where the mapping function $\mathbf{f}$ can be approximated linearly. Thus,

under the mapping $\mathbf{f}^{-1}$, the ellipse in $\bar{\mathbf{I}}$-space maps directly to another ellipse in $\mathbf{P}$-space. This new ellipse is centred on the point $\mathbf{p} = \mathbf{p}_0$ and represents all possible parameter vectors which could be recovered from the vector of image quotients $\bar{\mathbf{i}} = \bar{\mathbf{i}}_0$. The error associated with parameter recovery is obtained by considering the worst case scenario. That is, the point within the ellipse in $\mathbf{P}$-space which is at the maximum distance from the point $\mathbf{p} = \mathbf{p}_0$. This maximum distance must be calculated separately for each component, p_k, of the parameter vector to obain the error associated with recovery of each individual component. To calculate these errors it is necessary to consider how the ellipse is transformed under the mapping $\mathbf{f}^{-1}$, which is linear provided the Jacobian is non-zero.

Under a linear mapping the ellipse will be translated, scaled and rotated. The translation associated with the linear mapping defines the point $\mathbf{p} = \mathbf{p}_0$ which is mapped to from the point $\bar{\mathbf{i}} = \bar{\mathbf{i}}_0$. The two other transformations, scaling and rotation, are best understood by considering how a vector $d\bar{\mathbf{i}} = d\mathbf{f}$, in $\bar{\mathbf{I}}$-space, maps under $\mathbf{f}^{-1}$ to give a corresponding vector $d\mathbf{p}$ in $\mathbf{P}$-space. The vector $d\mathbf{p}$ can be calculated from the inverse form of equation (24) which, in matrix form, is given as

$$d\mathbf{p} = \mathbf{J}^{-1}\, d\bar{\mathbf{i}} \tag{25}$$

where $\mathbf{J}$ denotes the Jacobian matrix. Note that $\mathbf{J}^{-1}$ exists only if the Jacobian in non-zero. This must be the case if the 1-1 condition is to be satisfied.

The vectors $\mathbf{A}$ and $\mathbf{B}$ correspond to the major and minor axes of the ellipse in $\bar{\mathbf{I}}$-space and are given as

$$\mathbf{A} = \begin{pmatrix} \Delta\bar{i}_1 \\ 0 \end{pmatrix} \qquad \mathbf{B} = \begin{pmatrix} 0 \\ \Delta\bar{i}_2 \end{pmatrix}.$$

Under the mapping $\mathbf{f}^{-1}$ these vectors map to the vectors $\mathbf{A}'$ and $\mathbf{B}'$ which correspond to the major and minor axes of the ellipse in parameter space. Solving equation (25) for each of these vectors gives

$$\mathbf{A}' = \begin{pmatrix} \Delta p_1^A \\ \Delta p_2^A \end{pmatrix} \qquad \mathbf{B}' = \begin{pmatrix} \Delta p_1^B \\ \Delta p_2^B \end{pmatrix}$$

where Δp_1^A and Δp_2^A are the components of the vector A' in the direction of p_1 and p_2 respectively. Similarly Δp_1^B and Δp_2^B are the components of the vector B' in the direction of p_1 and p_2 respectively. To calculate the error in each component of the parameter vector it is necessary to consider the worse case scenario. It can be seen from figure 2 that this corresponds to taking the maximum of Δp_1^A and Δp_1^B as the error in p_1 and taking the maximum of Δp_2^A and Δp_2^B as the error in p_2. This error can be specified by a vector $\Delta\mathbf{p}$ and can be calculated for any given point in parameter space. With this measure of the accuracy of parameter recovery across the whole of parameter space, it is possible to define an optimisation criterion. This could simply be based on a sum of the errors at every point in $\mathbf{P}$-space or could be chosen to favour accuracy of recovery of a subset of the original

parameters. Once this optimisation criterion has been defined, a search can be used to find the optimum mapping function $\mathbf{f}$. It is important to note that, although the above discussion was based on a 2D parameter space, the methodology is equally applicable to any K dimensional parameter space.

An algorithm for the implementation of the proposed methodology is given as follows:

1. Establish a suitable search space from a parameterisation of mappings b and c.
2. For a given mapping function $\mathbf{f}$ calculate the vector of image quotients for each point within a discretised parameter space.
3. For each point, check that the Jacobian is either stricly positive or strictly negative across the whole of parameter space. If this condition is held then compute the inverse of the Jacobian matrix. If not then return to step 1 and define a new mapping function $\mathbf{f}$.
4. Using equation (19) calcuate the error associated with image acquisition for each vector of image quotients.
5. From the image quotient vector error calculate the maximum possible error in each component, p_k, of the parameter vector across the whole of parameter space.
6. Use the vector of parameter errors at each point within parameter space to measure the accuracy of parameter recovery.
7. Repeat steps 2-6 with some optimisation technique which enables an optimum mapping function $\mathbf{f}$ to be determined.

It is fairly straightforward to extend this methodology to the case in which $\bar{N} > K$, that is, where there are more image quotients than parameter values. Initially every possible K dimensional subspace of image quotients will need to be defined from the orignal $\bar{N}$ dimensional space of image quotients. It will then be necessary to go through the above procedure for each potential subspace and obtain the vector of parameter errors at each point within parameter space. To achieve the maximum possible accuracy the best $\Delta\mathbf{p}$ must be selected at every location within parameter space. Thus every point in $\mathbf{P}$-space will be linked to a specific image quotient combination. It will then be necessary to link every region of the original $\bar{N}$ dimesional space of image quotients to the particular subspace of image quotients which should be used for parameter recovery. It is important to note that it is necessary to recover the whole parameter vector at each point $\bar{\mathbf{i}}_0$ within a particular K dimensional subspace of image quotients. It is not possible to attempt to improve the accuracy of the system by recovering different components of the parameter vector from different K dimensional subspaces of image quotients. This is mathematically invalid.

6. Optimisation techniques

The mapping function f is a composite function of three separate mappings. Although the first mapping a, from parameter space to wavelength space, is fixed for a given problem, mappings b and c can vary depending on the choice of optical filters and definition of image quotients. Thus, to define an appropriate search space it is necessary to parameterise mappings b and c. Mapping b, which represents image acquisition, is defined by the positive $N \times M$ matrix R_m^n, given in equation (11). Typically this matrix will contain many elements and an appropriate parameterisation should be based on typical filter response functions. For example the position of the central wavelength and a measure of width could be used to define a Gaussian shape. Parameterisation of the mapping function c will be fairly straightforward as there are only a limited number of ways of combining image values to produce independent image quotients. In some applications the form of this mapping may be fixed a priori. Thus, it will not increase the overall dimensionality of the search space.

An optimisation method should search the whole space of possible mappings using the optimisation criterion outlined in the previous section. One technique which is ideally suited to this type of search is a genetic algorithm (GA)[20] as it is straightforward to define a fitness function which measures the accuracy of parameter recovery. Genetic algorithms have been shown to work well on a wide range of problems with objective functions that do not possess "nice" properties such as continuity, differentiability or satisfaction of the Lipschitz Condition.[21,22] This technique is used in the following section where an example application is discussed in detail.

7. Application: analysis of normal skin composition

7.A. Prediction of spectral reflectance

In order to perform mapping a it is necessary to have either a mathematical model which can predict spectral reflectance for a given set of parameter values or some technique for measurement of the appropriate spectrum. For this application we use the mathematical model developed by Cotton and Claridge.[18] With this model it is possible to predict the spectral reflectance for a given set of parameters. An outline of the model is now given.

Skin can be considered the four-layer structure depicted in figure 3. A negligible amount of light is reflected from the surface of the skin thus the surface term in equation (1) can be neglected. Although not absorbing any radiation, the stratum corneum scatters the incoming light in all directions. Light which penetrates this layer can thus be considered diffuse. In the epidermis light is absorbed by the pigment melanin. The absorption at each wavelength can be calculated using the Lambert-Beer law and will depend on the product of the melanin extinction coefficient and the pigment concentration. After passing through the epidermis the

light is both scattered and absorbed by the papillary dermis. The absorption results from the presence of blood and scattering from the underlying collagen structure. The simple Kubelka-Munk light theory[17] can be used to model the interaction of light with the papillary dermis as the necessary condition of diffuse incident illumination is satisfied. Any light which passes through the papillary dermis into the recticular dermis can be neglected as no significant backscattering occurs in this layer. Using this two-layer light transport model it is possible to obtain the remitted spectra for a given concentrations of melanin and blood. A more detailed description of this model can be found in reference.[18]

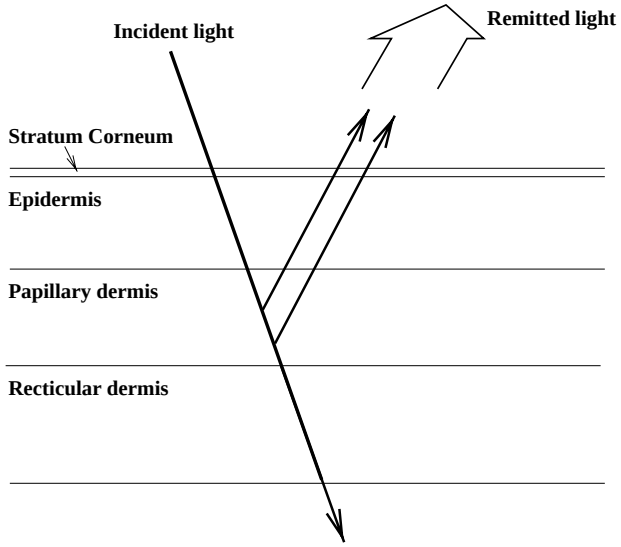

Fig. 3. Structure of normal skin

For a given papillary dermal thickness, changes in melanin and blood characterise all histological variation and thus define a 2-D parameter space for healthy skin. To carry out the optimisation proceedure developed in section 5 it is necessary to discretise parameter space. This is done at equal intervals to define 10×10 points, each of which correspond to a spectrum generated by the mathematical model. For simplicity, concentration values will be denoted by a number between 1 and 10. Figures 4a and 4b show how the remitted spectrum changes as melanin and blood are varied respectively.

With a change in melanin concentration the intensity of the whole spectrum is seen to decrease, with a more pronounced change in the blue region. As the blood concentration is decreased the most significant reduction in intensity is observed in the green region, the resulting shape reflecting the two absorption maxima of oxyhaemoglobin, a blood born pigment.

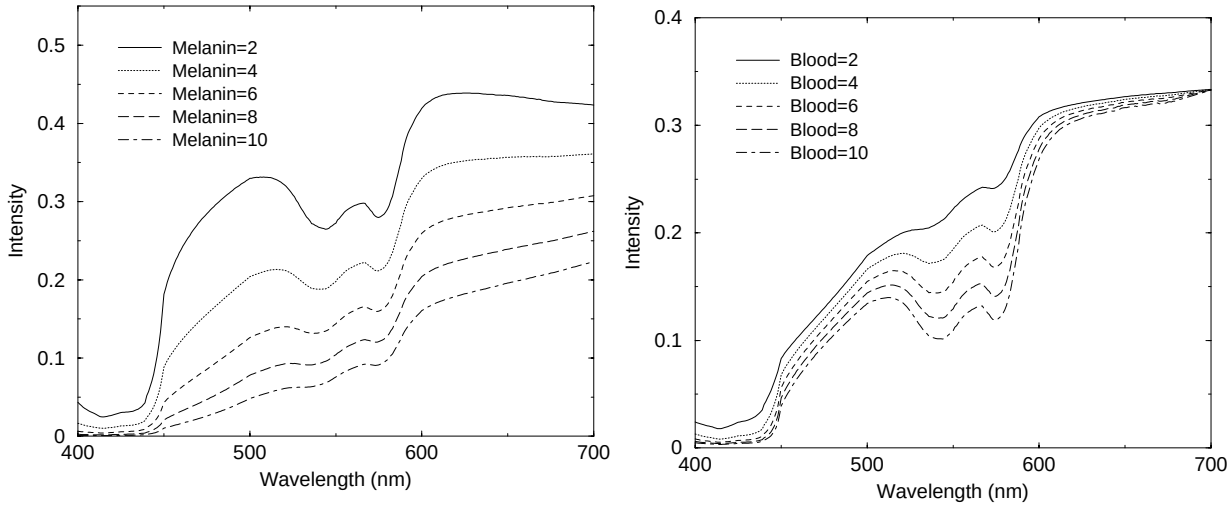

(a) (b)

Fig. 4. (a) Remittance spectrum of normal human skin for varying melanin concentration with blood concentration = 5. (b) Remittance spectrum of normal human skin for varying blood concentration with melanin concentration = 5.

7.B. Obtaining an optimum mapping function

To define a suitable search space it is necessary to parameterise the mappings b and c. A parameterised form of b is chosen to define a typical interference filter. This is modelled as a square profile with Gaussian decay at each side. Two parameters are required to specify this shape: the central wavelength and a full width half maximum (FWHM). Optimisation is carried out for three such filters, defining a 6-D search space. With three filters, i_1; i_2 and i_3, the only possible definition of image quotients, if we assume i_1/i_3 is equivalent to i_3/i_1, is given as

$$\bar{i}_1 = \frac{i_1}{i_3} \qquad \bar{i}_2 = \frac{i_2}{i_3}. \tag{26}$$

In this instance the mapping c does not increase the dimensionality of the search space.

The optimisation procedure was implemented following the algorithm given in section 5. Initially the vector of image quotients was calculated for every point within the discretised parameter space. This was done using the mathematical model to perform mapping a, the parameterised form of matrix R_n^m to perform mapping b and the equations (26) to perform mapping c. The derivative of each image quotient, with respect to each parameter, was obtained at each point within discretised parameter space using three-point finite-difference

approximations. The Jacobian matrix was then constructed at every point within parameter space, and providing its determinant was non-zero everywhere, the inverse calculated. If this condition was violated then a new mapping $\mathbf{f}$ was defined. The errors associated with image acquisition were then calculated using equation (19). The absolute value of the error in each image value will vary depending on the camera gain setting. Although this constant will not affect the mapping $\mathbf{f}$, it must be estimated in order to calculate the effective camera error. For this application is was taken to be 0.78% of the maximum value of all the image values across parameter space. This corresponds to a camera which has been set to give a maximum reading for the largest spectral reflectance and a camera error of two grey scale levels in a 8-bit representation.

Using the procedure outlined in section 5 the error associated with parameter recovery in both melanin and blood was obtained for each point within the discretised parameter space. In order to find an optimum $\mathbf{f}$, it is necessary to minimise the errors in recovery of both melanin and blood across the whole of parameter space. Thus the fitness function for the GA was taken to be the sum of the errors in both melanin and blood. This procedure was implemented in matlab using a standard GA to search the space of available mappings.

The boundaries of the search space were chosen such that the central wavelength was constrained to lie in the visible region (400nm-700nm) and such that the widths of the filters were allowed to vary from a FWHM of 25 to 200nm. Although it is now possible to engineer almost any shape of interference filter, this corresponds to a economically viable range of such filters.

7.C. Results and discussion

Although it was originally assumed that an image quotient defined as i_1/i_3 would be equivalent to i_3/i_1, the results of the GA seach showed that this was not the case. The search was intitialised for a random seed and, although the same central wavelengths were always obtained, different filters were selected corresponding to i_3 defined in (26). Further investigation showed that these local maxima in the search space corresponded to differing distributions of errors both, across parameter space and between the two parameters. This is because the fitness function, or measure of accuracy, was defined as the sum the errors across parameter space for both melanin and blood. Thus, a loss of accuracy in one parameter could be compensated for with an increase in the other. It may be that, with a more exact specification of the error distribution in the fitness function, it would be possible to obtain the same results for every GA search.

Figure 5 shows a filter combination which gave a similar error in the recovery of both melanin and blood.

The image quotients were calculated by dividing the filter centred at $\lambda = 473$nm and

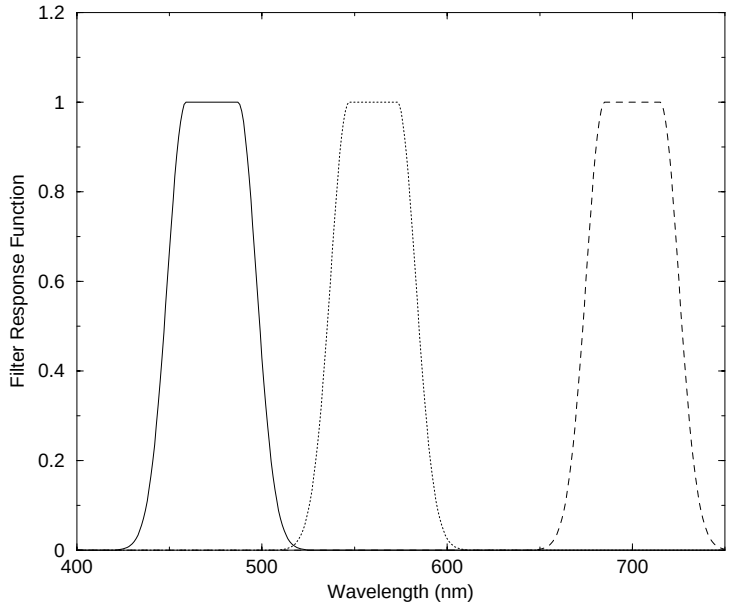

Fig. 5. Optimum filter response curves for extracting parameters which describe normal skin. The central wavelengths are 473nm, 560nm, 700nm

$\lambda = 560$nm by the response of the filter centred at $\lambda = 700$nm. To understand why these specific filters were selected it is necessary to analyse the spectral curves shown in figure 4. The filters centred at $\lambda = 473$nm and $\lambda = 560$nnmm correspond to spectral locations where there is a large change in intensity with the parameters melanin and blood respectively. A third filter was then required in a region of the spectrum in which the remitted light which was either significantly less or significantly more than that of the other two filters. The filter centred at $\lambda = 700$nm was chosen as it always gave the largest response at any point within parameter space. This ensured that the derivatives of each image quotient decreased monotonically across the whole of parameter space. The Jacobian, calculated from these derivatives, was stricly positive across the whole of parameter space. It is interesting to note that some alternative filter combinations gave Jacobians which were stricly negative across parameter space, corresponding to alternative local maxima in the search space. If two filters are chosen, to define an image quotient, which vary similarly across parameter space, there will be minimal change in that image quotient and thus it will be of limited value for parameter measurement.

Table 1 and Table 2 give the errors associated with recovery of melanin and blood respectively at every point within the discretised parameter space, for the filter combination given in figure 5. These errors have been calculated assuming a camera uncertainty of two grey scale levels in an 8-bit representation that is, an error of (2/255). The errors can be seen to

increase as both the melanin and blood concentrations increase. This is due to the decreasing effect on the final remitted spectrum of changing the pigment concentrations. Although this absolute error increases, the fractional error at each point actually decreases and it is nearly always possible to differentiate points in parameter space as the error rarely rises above 0.5.

	Melanin Concentration									
Blood Concentration	1	2	3	4	5	6	7	8	9	10
1	0.19	0.20	0.23	0.25	0.28	0.31	0.35	0.39	0.44	0.50
2	0.19	0.21	0.23	0.26	0.29	0.32	0.36	0.40	0.45	0.51
3	0.20	0.21	0.24	0.26	0.29	0.33	0.37	0.41	0.47	0.53
4	0.20	0.22	0.24	0.27	0.30	0.34	0.38	0.43	0.48	0.55
5	0.20	0.23	0.25	0.28	0.31	0.35	0.39	0.44	0.50	0.57
6	0.21	0.23	0.26	0.29	0.32	0.36	0.41	0.46	0.52	0.59
7	0.22	0.24	0.27	0.30	0.33	0.37	0.42	0.47	0.53	0.61
8	0.22	0.25	0.27	0.31	0.34	0.38	0.43	0.49	0.55	0.63
9	0.23	0.25	0.28	0.32	0.35	0.40	0.45	0.51	0.57	0.65
10	0.23	0.26	0.29	0.33	0.37	0.41	0.46	0.52	0.59	0.68

Table 1. Error associated with melanin recovery across parameter space

8. Conclusion

It has been demonstrated that, using an objectively defined set of optical filters, it is possible to recover scene parameters from image data in a way which is insensitive to geometry and incident illumination. In the example problem, discussed in the previous section, the error associated with this parameter recovery was found to be relatively small. The invariance of this mapping means that the technique will be particularly applicable to medical image applications where there is significant curvature of the surface of the imaged tissue, such as near a joint. It will also be unnecessary to calibrate the camera to determine the intensity of the incident light. This could help to significantly increase the speed of image aquisition and later processing.

The methodology outlined in this article has been developed for a measurement task, where the scene parameters are known to vary continuously. Work is currently being undertaken to extend the technique to problems of recognition, where it is necessary to differentiate discrete objects based on some measure of their spectral reflectance. This approach has

Blood Concentration	Melanin Concentration 1	2	3	4	5	6	7	8	9	10
1	0.25	0.27	0.28	0.30	0.32	0.34	0.36	0.38	0.40	0.43
2	0.26	0.28	0.29	0.31	0.33	0.35	0.37	0.40	0.42	0.45
3	0.27	0.29	0.31	0.33	0.35	0.37	0.39	0.42	0.44	0.47
4	0.29	0.31	0.33	0.35	0.37	0.39	0.42	0.44	0.47	0.50
5	0.31	0.32	0.35	0.37	0.39	0.42	0.44	0.47	0.50	0.54
6	0.32	0.34	0.37	0.39	0.42	0.44	0.47	0.50	0.54	0.57
7	0.34	0.37	0.39	0.42	0.44	0.47	0.50	0.54	0.57	0.61
8	0.37	0.39	0.42	0.44	0.47	0.50	0.54	0.57	0.61	0.66
9	0.39	0.42	0.44	0.47	0.51	0.54	0.58	0.62	0.66	0.70
10	0.42	0.45	0.48	0.51	0.55	0.58	0.62	0.66	0.71	0.76

Table 2. Error associated with blood recovery across parameter space

been used by Healey[10] who used the idea of normalised colour to identify different regions of normalised colour space corresponding to different metal and dieletic materials. This enabled geometry-insensitive segmentation of an imaged object comprised of a number of different materials.

Finally, it is important to note that in order to implement the proposed methodology, a look-up table must be established between all possible image quotients and scene parameters. Although this may be time consuming, it is only necessary to carry out this proceedure once. Once established, this look-up table will ensure no significant processing after image acquistion, making this technique particularly suitable to real-time applications.

Acknowledgments

The authors would like to acknowledge the help and guidance of Dr Jon Rowe.

References

1. B. K. P. Horn, "Obtaining shape from shading" in *Shape from Shading*, B. K Horn and M. J. Brooks, eds. (MIT Press, 1989).
2. G. Healey and D. Slater, "Using illumination invariant colour histogram descriptors for recognition" in *Proc. IEEE Computer Society Conference on Computer Vision and*

Pattern Recognition (Institute of Electrical and Electronic Engineers, Seattle, 1994), pp. 355–360.

3. S. J. Preece and E. Claridge, "An approach to physics-based vision using material specific spectral characterisation," submitted to IEEE trans. Patt. Anal. Mach. Int. (2001).
4. S. A. Shafer, "Using colour to separate reflection components," Col. Res. Appl. **10**, 210–218 (1985).
5. G. J. Klinker, S. A. Shafer and T. Kanade, "A physical approach to colour image understanding", Int. J. Comput. Vis." **4**, 7–38 (1990).
6. Q. Luong, "Colour in computer vision" in *Handbook of pattern recoginition and computer vision*, C.H. Chen, L.F. Pau and P.S.P. Wang, eds. (World Scientific Publishing Company, 1993).
7. G. Klinker, S. Shafer and T. Kanade, "Image segmentation and reflection analysis through color" in *Proceedings of the Image Understanding Workshop* (Morgan Kaufmann, California, 1988), pp. 838–853.
8. L. Maloney and B. Wandell, "Color constancy: a method for recovering surface spectral reflectance", J. Opt. Soc. Am. A **3**, 29–33 (1986).
9. D. B. Judd, D. L. MacAdam and G. Wyszecki, "Spectral distribution of typical daylight as a function of correlated color temperature," J. Opt. Soc. Am. A **54**, 1031–1038 (1964).
10. G. Healey, "Using colour for geometry-insensitive segmentation," J. Opt. Soc. Am. A **6**, 920–937 (1989)
11. G. Healey and T. O. Binford, "A color metric for computer vision" in *Proceedings of the IEEE conference on computer vision an pattern recognition* (nstitute of Electrical and Electronic Engineers, New York, 1988), pp. 10–17.
12. B. K. P. Horn, "Exact reproduction of colored images", Comput. Vis. Graph. Image Process **26**, 135–167 (1984).
13. B. Wandell, "The synthesis and anlysis of color images", IEEE trans. Patt. Anal. Mach. Intell. **PAMI-9**, 2–13 (1987).
14. M. A. Afromowitz, G. S. van Liew and D. M. Heimbach, "Clincal evaluation of burn injuries using an optical reflectance technique", IEEE trans. Biomed. Eng. **BME-34**, 114–127 (1987).
15. M. A. Afromowitz, J. B. Callis D. M. Heimbach, L. A. Desoto and M. K. Norton, "Mulitspectral imaging of burn wounds: a new clinical instrument for evaluating burn depth", IEEE tran. Biomed. Eng. **35**, 842–849 (1988).
16. S. A. Prahl, M. Keijzer, S. L. Jacques and A. J. Welch, "A monte carlo model of light propagation in tissue", SPIE Institue Series IS **5**, 102–111 (1989).
17. P. Kubelka and F Munk, "Ein Beitrag zur Optik der Farbanstriche", "Z. Tech. Opt" **11**, 593–611 (1931).

18. S. D. Cotton and E Claridge, "Developing a predictive model of human skin colouring," Proc. of SPIE Med. Imag. **2708**, 814–825 (1996).
19. M. M. Lipschutz, *Differential geometry*
(McGraw-Hill Book Company, New York, 1969)
20. T. Back and H. P. Schwefel, "An overview of evolutionary algorithms for parameter optimisation," Evolutionary Computation **1**, 1–23 (1993).
21. L. Davis, *The handbook of genetic algorithms*
(Van Nostrand Reingold, New York, 1991)
22. D. Goldberg, *Genetic algorithms in search, optimization and machine learning*
(Addison-Wesley, London, 1989).